SAND2022-14214C

The High-Resolution Wavelet Transform: A Generalization of the Discrete Wavelet Transforms

Miguel Jiménez-Aparicio*, Matthew J. Reno*, and John W. Pierre†
*Sandia National Laboratories, Albuquerque, NM, USA
†University of Wyoming, Laramie, WY, USA

***Abstract*—The development of the High-Resolution Wavelet Transform (HRWT) is driven by the need of increasing the high-frequency resolution of widely used discrete Wavelet Transforms (WTs). Based on the Stationary Wavelet Transform (SWT), which is a modification of the Discrete Wavelet Transform (DWT), a novel WT that increases the number of decomposition levels (therefore increasing the previously mentioned frequency resolution) is proposed. In order to show the validity of the HRWT, this paper encompasses a theoretical comparison with other discrete WT methods. First, a summary of the DWT and the SWT, along with a brief explanation of the WT theory, is provided. Then, the concept of the HRWT is presented, followed by a discussion of the adherence of this new method to the WT's common properties. Finally, an example of the application is performed on a transient waveform analysis from a power system fault event, outlining the benefits that can be obtained from its usage compared to the SWT.**

***Index Terms*—Digital Signal-Processing, Wavelet Transforms, Digital Filter Design, Time-Frequency Decomposition**

I. Introduction

Time-frequency analysis tools are used in many different fields that may need to study non-stationary signals. Over the last few decades, the number of available mathematical tools and capabilities has been largely expanded by a committed research community. The beginning of this field starts with the Short-Time Fourier Transform (STFT), proposed by D. Gabor in 1946, which aims to overcome the limitations of the Fourier Transform (FT) [1]. Basically, the FT aims to define the frequency spectrum of a stationary signal over a period of time. The FT uses sine waves of different frequencies to analyze a signal. Therefore, the signal is represented through a linear combination of sine waves [2]. However, it doesn't provide any detail about when each of the frequency components were present in the signal. By applying the FT over short time windows instead, it is possible to capture local frequency variations in the signals. However, this approach is not as convenient as different signals can have the same Fourier domain representation, and there is a trade-off between time and frequency resolution [3]. A narrow time window will result in a good time resolution but on a poor frequency resolution. Whereas a wide-time window will result in a good frequency resolution but in a deficient time resolution and, therefore, it will not be possible to distinguish the local changes of frequency [4]. The employed window is the same for all frequencies, and if several resolutions are required, the STFT operation has to be repeated for several window lengths [5]. Following the path of the SFTF, other approaches were proposed, such as the Wigner-Ville Distribution (WVD) function [1]. This technique applies the STFT to the signal autocorrelation function. This gives a high-resolution time-frequency representation of a signal, but the results are difficult to interpret due to the appearance of cross terms. In those cases, a smoothed WVD pseudo version is preferred [6].

However, the rise of Wavelet Transforms (WTs) has hoarded the attention of researchers in the last four decades. Many applications use them [7], such as: audio and image compression, signal denoising, feature extraction, etc. The concept of "wavelet" was first introduced by J. Morlet in 1982 for geophysical applications [8]. In these transforms, the signal is decomposed on a base of functions called "daughter wavelets" or simply, "wavelets", which are scaled and shifted copies of a mother wavelet. Compared to the STFT, WTs varies simultaneously frequency and time scales resolution, increasing the time-frequency analysis capabilities [4]. Over the years, several researchers have made important contributions that have expanded the WT theory and applications. In this regard, the work of I. Daubechies and R. Coifman in the development of new wavelet families is especially remarkable [9], [10].

The most common types of WTs are the Continuous Wavelet Transform (CWT) and the Discrete Wavelet Transform (DWT). The CWT performs multiple convolutions of the input signal over time and a defined set of wavelets. Each daughter wavelet draws information about specific frequency components of the input signal. A matrix of coefficients is obtained where the y-axis corresponds to the "scales" (inversely related to the frequency components, so the first scale corresponds to the highest frequency component in which the signal can be decomposed) while the x-axis is time. The main drawback of the CWT is that it has a large redundancy of information when it comes to the signal reconstruction, which implies more computation time and resources. The Stockwell transform (or S-transform) was developed in mid-1990s and conceptually is a generalization of the STFT. Instead of the

M. Jiménez-Aparicio and M.J. Reno are with the Electric Power Systems Research Department at Sandia National Laboratories, Albuquerque, NM (email: mjimene@sandia.gov). This material is based upon work supported by the Laboratory Directed Research and Development program at Sandia National Laboratories and the U.S. Department of Energy's Office of Energy Efficiency and Renewable Energy (EERE) under Solar Energy Technologies Office (SETO) Agreement Number 36533. Sandia National Laboratories is a multimission laboratory managed and operated by National Technology and Engineering Solutions of Sandia, LLC., a wholly owned subsidiary of Honeywell International, Inc., for the U.S. Department of Energy's National Nuclear Security Administration under contract DE-NA0003525.

fixed window, it is based on a moving and scalable localizing Gaussian window. The S-transform lies close to the CWT, providing a certain phase correction to this transform [11].

Nevertheless, the discrete WTs present a more optimum approach. In this group, both the previously mentioned DWT and the Stationary Wavelet Transform (SWT) are included. Proposed by S. Mallat in the 1980s, the approach is to decompose the signal in successive frequency bands using multirate filter banks [12]. This is known as Multi-Resolution Analysis (MRA) or "subband coding" [13]. The base case employs two-channel critically sampled filter banks in each decomposition level, which actually gives the lowest number of coefficients that is required for a perfect reconstruction (very desirable for compression tasks) [14]. The SWT is a modification of the DWT which provides some advantages of its counterpart. First it is shift-invariant, which is desirable for time-series analysis. Second, all sets of coefficients have the same length, which may ease their interpretation.

The development of the WTs continued, and the second generation of WTs appeared at the end of the 1990s [15]. This new group of transforms aims to maintain the same time-frequency decomposition properties, but adapt them to overcome some traditional assumptions about the infinity of the signals. The concept behind this revision is to split the signals into two groups: even and odd samples, and try to predict the odd samples using the even ones. This assumes that consecutive samples are highly correlated in digital signals, and that the local signal structure can be predicted [16]. Even though the concept sounds promising, they never achieved the popularity of the first generation of WTs.

The purpose of this paper is to propose a new modification of other discrete WTs that aims to provide a larger amount of decomposition levels, and which is especially suitable for time-frequency signal representation of high-frequency signals. In comparison to others WTs, the HRWT aims to reduce the spread of the frequency bands (in practice, this means to increase the number of decomposition levels) to achieve a finer frequency decomposition. The rest of the paper is organized as follows: Section II explains in detail the concepts of DWT and SWT, Section III explains the theory behind the WTs, Section IV shows how this theory is adapted on the HRWT. Next, Section V compares the results for the HRWT and the SWT. Section VI includes a discussion of other methods that could draw a similar result to the HRWT. Finally, the conclusions of this paper are gathered in Section VII.

II. Background

This section aims to explain the basics of the discrete WTs, namely the DWT and the SWT, on top of which the HRWT is designed. In order to understand the novelty of the new proposed transform, it is necessary to understand the method behind the DWT and SWT. The DWT will be explained first, followed by a second subsection that details the changes introduced in the SWT.

A. The Discrete Wavelet Transform (DWT)

As mentioned before, the implementation of the DWT is similar to sub-band filtering or filter banks, in which the signal goes through a series of filters that extract the frequency components in the corresponding frequency sub-band. This resembles a tree structure, as can be observed in Fig. 1. In this example, the sampling frequency (F_s) is 10 MHz.

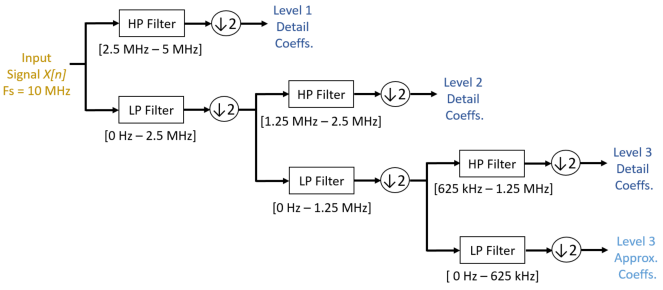

Fig. 1: DWT structure for 3 decomposition levels

In each level, the input signal is convoluted by the coefficients of a pair of half-band high-pass (H_p) and low-pass (L_p) filters, returning a set of "detail" and "approximation" coefficients. It is important to note that, in the discrete WTs, the mother wavelet is interpreted as a (continuous) filter impulse response [14]. These filter coefficients depend on the wavelet family and order. The mathematical operation of convolution is defined as follows:

$$x[n] * f[n] = \sum_{k=-\infty}^{\infty} x[k] \cdot f[n-k], \tag{1}$$

where $x[n]$ is the input signal and the $f[n]$ is the impulse response of the filter. In the DWT, there are two main aspects to note: decrease of the cut-off frequency, and decrease of the output signal length by two, both as the level of decomposition increases. The first observation is achieved by applying half-band filters. For a sampling frequency of 10 MHz, the maximum frequency component that we can expect to be contained by the measured signal is 5 MHz (without aliasing). In the first level, the high-pass filter output, which correspond to the detail coefficients of the first level of decomposition, is going to cover the frequency range of 2.5 MHz up to 5 MHz. The output of the low-pass filter contains all the frequency components from 0 to 2.5 MHz. By continuing the process, the maximum frequency in the frequency band is consecutively divided by 2. The resulting frequency bands for the detail coefficients can be observed in Table I.

TABLE I: Boundaries for the Frequency Bands

Decomposition Level	Lower Frequency	Upper Frequency
1	2.5 MHz	5 MHz
2	1.25 MHz	2.5 MHz
3	625 kHz	1.25 MHz
4	312.5 kHz	625 kHz
5	156.25 kHz	312.5 kHz
6	78.125 kHz	156.25 kHz

The second observation can be explained by taking into account the Nyquist-Shannon Theorem. In sub-band filtering, the filtering process is accompanied by a down-sampling of the signal. This occurs because, as in each decomposition level the maximum frequency is divided by two, the required sampling frequency can be halved as well without loss of information. In practice, this means that as the level of decomposition increases, the length of the output signals decreases with a rate of a power of two (one of every two samples is dropped in each decomposition level as it is not necessary). Therefore, this leads to a poorer time resolution, as any event which was accurately represented in a full-length input signal has to be represented in a smaller number of coefficients in each new level. Referring to the half-band high-pass filter as $h[n]$, and the half-band low-pass filter as $g[n]$, the output of a new decomposition level can be expressed as follows:

$$y_{high}[n] = \sum_k x[k] \cdot h[2k - n], \tag{2}$$

$$y_{low}[n] = \sum_k x[k] \cdot g[2k - n], \tag{3}$$

where $x[n]$ is the input of that decomposition level and $y_{high}[k]$ and $y_{low}[k]$ are the set of output signals. The election of a downsampling rate of 2 is not arbitrary. It comes from the concept of Perfect Reconstruction (PR) filter banks, in which the signal is decomposed in M frequency bands with M different channels, while a downsampling of rate N is applied to each channel in order to avoid aliasing [14]. Afterwards, the signal is reconstructed by upsampling at a rate N and applying the synthesis filters. It is important to highlight that this is exactly the same process that would be needed for the reconstruction of the signal out of the DWT coefficients. A PR filter bank with 2 channels can be observed in Fig. 2.

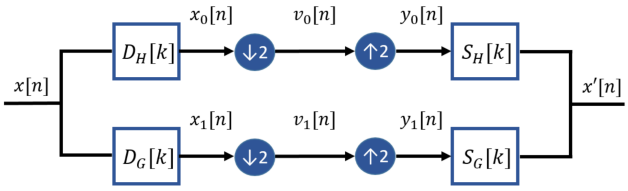

Fig. 2: Two-channel PR filter structure

$D_H[n]$ and $D_G[n]$ are the high-pass and low-pass decomposition filters, respectively, and $S_H[k]$ and $S_G[k]$ are the corresponding synthesis filters. Technically, the input and the output should be exactly the same signal. The difference is that, in the DWT, the filtering process is done on a tree structure, while on a PR filter bank it is done at the same level. In filter banks, the general rule is that the downsampling rate N has to be less or equal to the number of channels M. For some applications, especially in audio compression, the filter needs to have the lower possible number of channels (which the lowest non-trivial response is 2) in order to reduce the number of outputs. Therefore, the downsampling rate in this case has to be the same as the number of channels (which gives $M = N$). Filter configurations that fulfill the condition of $M = N$ are usually called "critically sampled filter banks". These filters gives the maximum available rate of downsampling that still allows to perfectly reconstruct the signal. The DWT, using 2 channels (in a tree structure) and a downsampling rate of 2, provides the smallest number of coefficients that are needed to represent and reconstruct the signal. A downsampling rate of 2 forces to use half-band filters in each decomposition level.

B. Stationary Wavelet Transform (SWT)

For the SWT, the structure is also similar to sub-band filtering: signals enter each decomposition level and go through a low-pass and high-pass filter. However, the SWT applies scaling in a different way. Instead of filtering and then downsampling the signal in each level, the SWT upsamples the filters using zeroes [17]. The cut-off frequency of the filters is modified by this procedure and there is no need for downsampling. Therefore, the length of the signal remains constant in all the levels. This offers an interesting property in time-series analysis: it is shift-invariant. Therefore, two identical signals but shifted in the time domain (for example, if padded with zeroes) would lead to the same transformed time (taking into account that there is a delay). The DWT, however, is not shift-invariant and would lead to different results for shifted signals [18]. This is related to the downsampling or decimation process that takes place on every level. The frequency information is retained on some coefficients that are halved in each new decomposition level. Two identical signals but shifted in time would be downsampled in a different way, leading to different decomposition coefficients. The block diagram for the SWT is shown in Fig. 3.

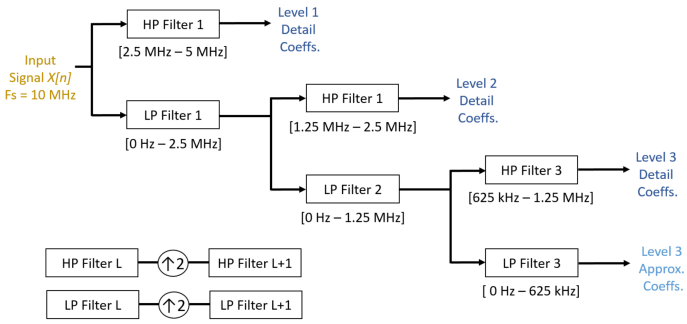

Fig. 3: SWT decomposition structure for 3 levels

The filters are upsampled by inserting zeroes between the filter coefficients. In order to recursively reduce the cut-off frequency by 2 in each decomposition level, the number of zeroes is increased exponentially by 2 following this series:

$$num\ 0s\ SWT\,(L) = 2^L - 1, \tag{4}$$

where L is the number of decomposition level. Therefore, for the first level, no zeroes will be introduced. For the

second level, just one zero will be introduced between the filter coefficients. For the third level, three zeroes will be the separation between the original filter coefficients, etc.

III. The Wavelet Transform Theory

The theory in this section is based on [19]. Formally, the discrete WTs can be defined, in a very simplified manner, as a two-parameter linear expansion that depends on scale j and translation coefficient k. In the following expression,

$$f(t) = \sum_{j,k} a_{j,k}\psi_{j,k}(t), \tag{5}$$

the term $a_{j,k}$ refers to the set of the detail coefficients plus the last approximation coefficients, while $\psi_{j,k}$ refers to the wavelet functions (i.e., the scaled daughter wavelets). It is important to note that the $\psi_{j,k}$ form an orthonormal basis for all j and k. Even though non-orthonormal wavelet basis do exist, MRA approaches are benefited from a simpler coefficient calculation and the fulfillment of the Parseval's Energy (PE) Theorem when orthonormal basis are employed. In order to clarify the notation in regard to scaling, the scale j is opposite to the term "decomposition level". Therefore, the first decomposition level actually refers to the largest scale (which produces the sharpest wavelets).

A more general expression for the DWT is:

$$f(t) = \sum_{j,k} a_{j,k}2^{j/2}\psi(2^j t - k), \tag{6}$$

where the daughter wavelets are actually computed by scaling the mother wavelet ψ. This scaling is done at an exponential rate to take into account the downsampling by a factor of 2. Note that 2^j is the scaling of t (j is the $\log_2$ of the scale), 2^{-jk} is the translation in t, and $2^{j/2}$ maintains the (perhaps unity) L^2 norm of the wavelet at different scales. This is efficiently implemented using MRA. A general expression can be found in the following equations:

$$f(t) = f_{j_0}(t) + \sum_{j} f_j(t), \tag{7}$$

$$f_{j_0}(t) = \sum_{k} c_{j_0}(k)2^{j_0/2}\varphi(2^{j_0}t - k), \tag{8}$$

$$f_j(t) = \sum_{k} d_j(k)2^{j/2}\psi(2^j t - k), \tag{9}$$

where $f_{j_0}(t)$ defines the lower frequency part of the signal $f(t)$, which is represented by the set of last approximation coefficients c_{j_0}. Similarly, $f_j(t)$ stands for the several decomposition levels in which the signal $f(t)$ is successively decomposed for each scale j, and d_j are the detail coefficients that define those signals in the wavelet basis. Finally, φ and ψ are the scaling and wavelet functions, respectively. The scaling function φ is related to the low-pass filtering procedure and, according to the MRA theory, it is obtained first. Then, the wavelets functions $\psi_{j,k}$ are designed on top of that ensuring that orthonormality is maintained. Orthonormality is a requirement for the PE theorem, which states that there is a relationship between the energy in both the time domain and frequency domains, as shown in:

$$\sum_{n=0}^{N-1} |x[n]|^2 = \frac{1}{N}\sum_{k=0}^{N-1} |X[k]|^2, \tag{10}$$

where $X[k]$ is the N-point Discrete Fourier Transform (DFT) of $x[n]$. Therefore, a (very desirable) consequence of the PE theorem is that, if the scaling functions and wavelets form an orthonormal basis, the energy of the signal $f(t)$ can be related to the energy in each of the components and their wavelet coefficients as defined in the following expression:

$$\int |f(t)|^2 dt = \sum_{l=-\infty}^{\infty} |c(l)|^2 + \sum_{j=0}^{\infty}\sum_{k=-\infty}^{\infty} |d_j(k)|^2. \tag{11}$$

The scaling function for a given scale j is a linear combination of the shifted versions of the scaling function at the next scale (i.e., higher frequency components), as it can be observed in:

$$\varphi(2^j t - k) = \sum_{n} g(n)\sqrt{(}2)\varphi(2^{j+1}t - 2k - n), \tag{12}$$

where $g(n)$ represents the low-pass filter coefficients. This satisfies the conceptual condition for MRA that requires that lower frequency components can be explained using larger frequency components. A similar expression could be derived for the wavelet functions $\psi_{j,k}$ but using both the high-pass filter coefficients $h(n)$ and the low pass filter coefficients $g(n)$, as the relationship is not direct. If these concepts are translated to (8)-(9), the following relationship between coefficients can be established:

$$c_{j+1}(k) = \sum_{m} c_j(m)g(k-2m) + \sum_{m} d_j(m)h(k-2m) \tag{13}$$

$$c_j(k) = \sum g(m-2k)c_{j+1}(m) \tag{14}$$

$$d_j(k) = \sum_{m} h(m-2k)c_{j+1}(m). \tag{15}$$

These equations reveal the importance of the correct design of the filter coefficients $g(n)$ and $h(n)$, and the importance of the downsampling by 2 as part of the scaling process in the DWT. As it was explained before, in the SWT the scaling process is the upsampling of the filter coefficients introducing zeroes. In this regard, the novelty introduced in the HRWT is that the filter coefficients are kept the same, but the upsampling process does not strictly follow a rate of 2.

IV. The High-Resolution Wavelet Transform (HRWT)

A. The concept

In the HRWT, the upsampling rate is left to the designer criteria, and it is not required to follow a specific pattern. The general expression of the HRWT is as follows:

$$f(t) = \sum_{j,k} a_{j,k} \psi(\nu(j)t - k), \tag{16}$$

where $\nu(j)$ stands for the custom upsampling rate per scale. As it is going to be shown later, the usage of a rate less than 2, but with the same filter coefficients, leads to the splitting of the former frequency into tighter bands (or "sub-frequency bands"). As a clarification, the composition of $\nu(j)$ is related to the desired inserted number of zeroes:

$$\nu(j) = num\ 0s\ HRWT\,(j) + 1, \tag{17}$$

where j is the scale. The maximum number of sub-frequency bands is achieved when the rate of inserted zeroes grows just by 1 zero per additional decomposition level. However, although this gives the maximum frequency resolution, it may not be useful for a moderately large number of equivalent SWT levels. Therefore, the content of $\nu(j)$ is left to design criteria. Maximum resolution can be used in the levels of interest, and then the rate of 2 (or even larger) can be used for the rest of the levels to save computation resources. Table II shows how the maximization works for up to the equivalent SWT Level 4, and then comes back to the original frequency band resolution (as in the SWT).

TABLE II: SWT and HRWT Equivalence

SWT Level	Num 0s SWT	HRWT Level	Num 0s HRWT
1	0	1	0
2	1	2	1
3	3	3	2
		4	3
4	7	5	4
		6	5
		7	6
		8	7
5	15	9	15

As it can be seen, SWT Levels 1 and 2 already had the maximum frequency resolution. So, the HRWT starts to make a difference at equivalent SWT Level 3.

B. Validation

The HRWT complies with the most important properties that are common to WTs (A full description of these properties and proofs can be found in [19]). This is in part achieved because the filter coefficients are kept the same as in the default discrete WTs. Regarding the filter coefficients, these properties are fulfilled:

$$\sum_n h(n) = \sqrt{2} \tag{18}$$

$$\sum_n |h(n)|^2 = 1 \tag{19}$$

$$\sum_n h_1(n) = 0. \tag{20}$$

Regarding orthonormality, the following properties have to be satisfied:

$$\sum_n h(n)h(n-2k) = \delta(k) = \begin{cases} 1 \text{ if } k = 0 \\ 0 \text{ otherwise} \end{cases} \tag{21}$$

$$\sum_n h(n)h_1(n-2k) = 0 \tag{22}$$

$$h_1(n) = \pm(-1)^n h(N-m), \tag{23}$$

where N is an arbitrary odd integer. It has been checked that they still hold for an arbitrary number of inserted zeroes.

V. The use case

In order to show the application of the HRWT decomposition in an actual signal, a wide-band power system fault event signal is used as an example. The signal is shown in Fig. 4.

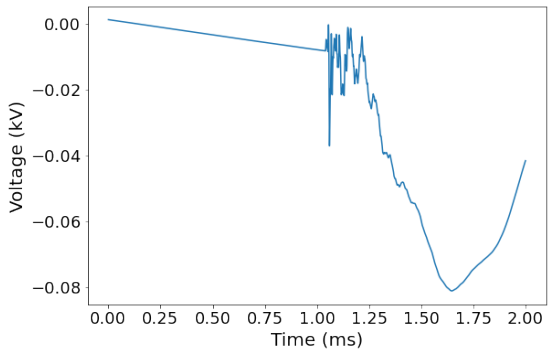

Fig. 4: Signal to decompose

This section is divided into three parts. In the first one, there is a comparison of the filters between the HRWT and the SWT. Secondly, the signal is decomposed into 5 equivalent SWT levels using both the SWT and the HRWT, and the respective coefficients are shown. In the case of the HRWT, the maximum resolution is going to be used up to equivalent SWT Level 4. Therefore, equivalent SWT Level 5 employs again the exponential rate. Finally, the reconstruction errors following the inverse process to recover the original signal are compared.

A. Filter coefficients comparison

In each decomposition level, there is a set of half-band high-pass and low-pass filters. In the case of the SWT, the cut-off frequency is halved in each consecutive level. In the HRWT, the newly generated intermediate levels also show an intermediate cut-off frequency. This leads to the set of frequency responses shown in Fig. 5.

However, in the end what really matters for the decomposition is what comes of combining these filters together. For example, the overall filter that gives the detail coefficients in SWT Level 3 is the combination of the low-pass filters in Level 1 and 2, and the high-pass filter in Level 3. Looking at these combinations, the frequency responses in Fig. 6 can be obtained. The same approach is applied to the HRWT filters.

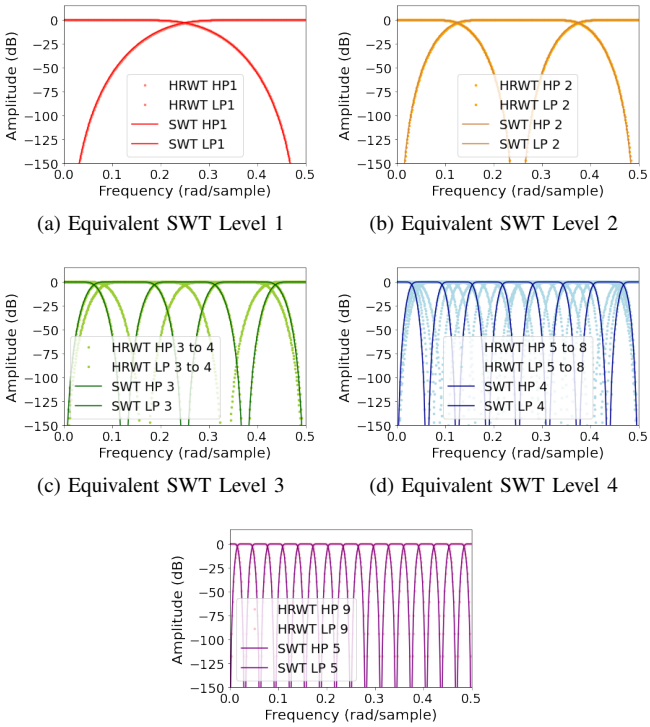

(a) Equivalent SWT Level 1

(b) Equivalent SWT Level 2

(c) Equivalent SWT Level 3

(d) Equivalent SWT Level 4

(e) Equivalent SWT Level 5

Fig. 5: Comparison of filters' frequency response

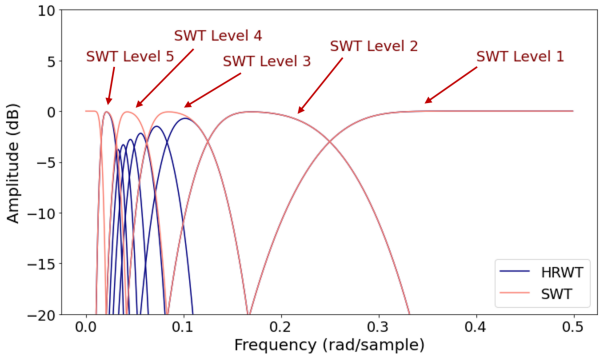

Fig. 6: Comparison of decomposition frequency bands

It becomes evident that the HRWT is dividing the former frequency bands of SWT Levels 3 and 4 into sub-frequency bands, providing additional resolution. SWT Levels 1 and 2 remain unchanged. For equivalent SWT Level 5, the rate is exponential again with a factor of 2, so there is no difference between the HRWT and the SWT. What is on the left-hand side of the SWT Level 5 is the low-pass filter response at that decomposition level, which gives the last approximation coefficients.

B. Decomposition coefficients comparison

Fig. 7 shows a level-wise comparison of the detail and last approximation coefficients for the SWT and the HRWT.

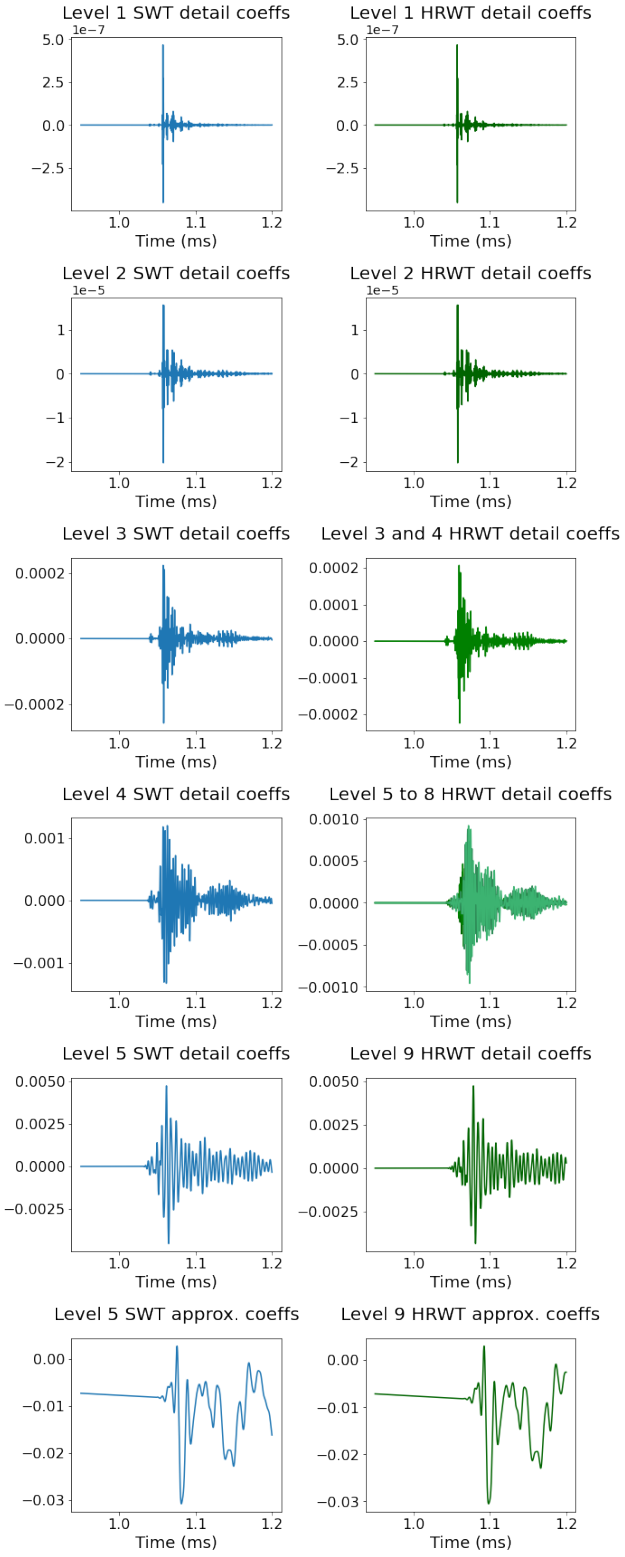

Fig. 7: Comparison of decomposition coefficients

The coefficients for Level 1 and 2 in both transforms are the same, which makes sense with the filter frequency response previously shown in Fig. 6. In SWT Level 3 and 4, the

overall magnitude of the coefficients is similar to the ones of the equivalent HRWT levels. This is coherent, since both transforms are working with the same frequency bands. The difference is that the HRWT divides this band into several sub-bands for further analysis. For SWT Level 5 and HRWT Level 9, even though they work with the same frequency band and the filter response should be the same, some slight differences can be appreciated in the coefficients. This is due to the fact that the inputs, which for one is the approximation coefficients of SWT Level 4, meanwhile for the other one is the approximation coefficients of HRWT Level 8, are not exactly the same. Therefore, the numerical values do not match perfectly. The same observation applies for the last set of approximation coefficients.

C. Signal reconstruction

One property of the WTs is that they are easily invertible. This means that the original signal can be recovered without a significant loss (just small numerical errors during the calculations) if the process is repeated backwards using the synthesis filters instead. In this section, the error introduced by the HRWT is compared to the case of the SWT. The error is calculated as the difference between the original signal and the reconstructed signal. As it can be seen in Fig. 8, the errors for both transforms are practically negligible and very close. The fact that the HRWT introduces a larger error can be explained by the decomposition in a larger number of levels.

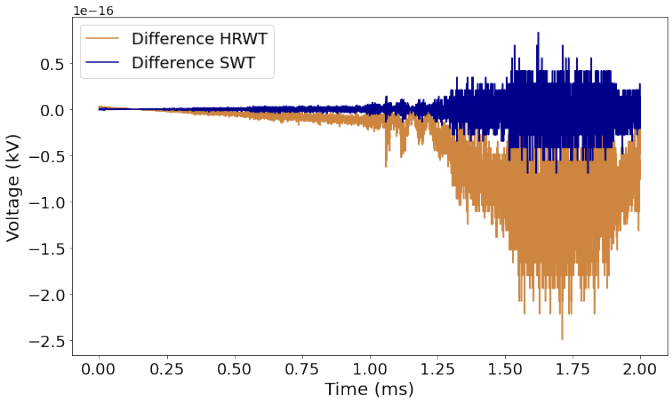

Fig. 8: Comparison of decomposition frequency bands

VI. Discussion

Other methods for achieving a larger decomposition of the default energy bands, such as Wavelet Packet Decomposition (WPD) or M-band decomposition (in opposition to just using 2 channels) have been proposed [19]. The HRWT doesn't aim to provide better decomposition capabilities. It is just another method to achieve these extra decomposition levels. In fact, those methods would split Levels 1 and 2, which is something that the HRWT cannot do. However, the HRWT is able to further split the other frequency bands. Actually, the principle shown in the HRWT can be combined with the aforementioned method to achieve even a more detailed decomposition.

VII. Conclusions

The Wavelet Transform (WT) that is proposed in this paper, called the High-Resolution WT (HRWT), provides additional frequency decomposition, in selected levels, compared to other discrete WT, such as the Discrete WT (DWT) or the Stationary WT (SWT). This is done by modifying the filter scaling method defined in the SWT by maximizing the number of inserted zeroes among consecutive levels, which leads to the splitting of former decomposition levels into several new sub-levels. The capabilities of the method have been validated on a wide-band signal from a power system fault event. In addition, it has been shown that the decomposed signal can be reconstructed back without a significant error. Therefore, the HRWT achieves the goal of expanding the decomposition capabilities of other discrete WTs in those frequency bands where additional decomposition is needed.

References

[1] L. Debnath and J.-P. Antoine, "Wavelet Transforms and Their Applications," *Physics Today - PHYS TODAY*, vol. 56, p. 68, 2003.

[2] G. B. Folland, *Fourier analysis and its applications*. Wadsworth Brooks/Cole Advanced Books Software, 1992.

[3] A. Tashakkori, P. J. Wolfs, S. Islam, and A. Abu-Siada, "Fault Location on Radial Distribution Networks via Distributed Synchronized Traveling Wave Detectors," *IEEE Transactions on Power Delivery*, vol. 35, no. 3, pp. 1553–1562, 2020.

[4] A. S. Bretas, R. H. Salim, and K. R. C. de Oliveira, "Fault detection in primary distribution systems using wavelets," in *International Conference on Power Systems Transients (IPST)*, 2007.

[5] Z. Wang, S. McConnell, R. Balog, and J. Johnson, "Arc fault signal detection - Fourier transformation vs. wavelet decomposition techniques using synthesized data," in *2014 IEEE 40th Photovoltaic Specialist Conference, PVSC 2014*, 2014.

[6] Mathworks, "Wigner-Ville distribution and smoother pseudo Wigner-Ville distribution."

[7] M. Sifuzzaman, M. Islam, and M. Ali, "Application of Wavelet Transform and its Advantages Compared to Fourier Transform," *J. Phys. Sci*, vol. 13, 2009.

[8] J. Morlet, G. Arens, E. Fourgeau, and D. Glard, "Wave propagation and sampling theory—Part I: Complex signal and scattering in multilayered media," *GEOPHYSICS*, vol. 47, no. 2, pp. 203–221, 1982.

[9] I. Daubechies, "Orthonormal bases of compactly supported wavelets," *Communications on Pure and Applied Mathematics*, vol. 41, pp. 909–996, oct 1988.

[10] R. Coifman, Y. Meyer, and M. Wickerhauser, "Wavelet analysis and signal processing," in: Wavelets and Their Applications," *Jones and Bartlett*, pp. 153–178, 1992.

[11] R. G. Stockwell, L. Mansinha, and R. P. Lowe, "Localization of the complex spectrum: the S transform," *IEEE Transactions on Signal Processing*, vol. 44, no. 4, pp. 998–1001, 1996.

[12] S. G. Mallat, "A theory for multiresolution signal decomposition: the wavelet representation," *IEEE Transactions on Pattern Analysis and Machine Intelligence*, vol. 11, no. 7, pp. 674–693, 1989.

[13] R. Polikar, "Multiresolution Analysis: The Discrete Wavelet Transform."

[14] M. Vetterli and J. Kovacevic, *Wavelets and subband coding*. No. BOOK, Prentice-hall, 1995.

[15] W. Sweldens, "The Lifting Scheme: A Construction of Second Generation Wavelets," *SIAM Journal on Mathematical Analysis*, vol. 29, pp. 511–546, mar 1998.

[16] W. Sweldens, "Wavelets and Digital Geometry Processing," in *IMA 20th Anniversary Conference*, 2003.

[17] M. Holschneider, R. Kronland-Martinet, J. Morlet, and P. Tchamitchian, "A Real-Time Algorithm for Signal Analysis with the Help of the Wavelet Transform," pp. 286–297, 1990.

[18] Mathworks, "Nondecimated Discrete Stationary Wavelet Transforms (SWTs)."

[19] C. S. Burrus, R. A. Gopinath, and H. Guo, "Wavelets and Wavelet Transforms," 1998.